

# Contrasting interannual variability of atmospheric moisture over Europe during cold and warm seasons

By IGOR I. ZVERYAEV<sup>1\*</sup>, JOANNA WIBIG<sup>2</sup> and RICHARD P. ALLAN<sup>3</sup>, <sup>1</sup>*P.P. Shirshov Institute of Oceanology, RAS, 36, Nakhimovskiy Ave., Moscow, Russia;* <sup>2</sup>*Department of Meteorology and Climatology, University of Łódź, Łódź, Poland;* <sup>3</sup>*Environmental Systems Science Centre, University of Reading, Reading, UK*

(Manuscript received 6 April 2007; in final form 4 October 2007)

## ABSTRACT

Seasonality in the interannual variability of atmospheric moisture over Europe is investigated using precipitable water (PW) from the National Centers for Environmental Prediction/National Center for Atmospheric Research reanalysis data set for 1979–2004. Over Europe the summer PW and its interannual variability (expressed by standard deviations) are essentially larger than those of the winter season. The largest seasonal differences are found over eastern Europe and European Russia, where the summer PW climatology and magnitudes of its interannual variability exceed respective winter characteristics by a factor of 2.5–3.8.

The first and second empirical orthogonal function (EOF) modes of winter PW over Europe are associated, respectively, with the North Atlantic Oscillation (NAO) and the East Atlantic teleconnection pattern. During summer the leading EOFs of PW are not linked to the known regional teleconnection patterns. Our analysis revealed that EOF-1 of summer PW is associated with sea level pressure (SLP) pattern characterized by two action centres of opposite polarity over northwestern Siberia and over a broad region including southern Europe, the Mediterranean Sea and part of northern Africa. The EOF-2 of summer PW is associated with cyclonic/anticyclonic SLP anomalies over Scandinavia and southwestern Europe.

It is shown that PW and precipitation variability are positively coupled during the cold season but not for the warm season. Instead, during the warm season we found a significant link between regional PW and air temperature variability, indicating an important role of local heating in variability of summer PW over Europe.

## 1. Introduction

It is well known that during the cold season the North Atlantic Oscillation (hereafter NAO) is the major driver of the European climate variability (e.g. van Loon and Rogers, 1978; Rogers, 1984; Hurrell, 1995; Seager et al., 2000). Since the NAO is linked to sea surface temperature variations in the North Atlantic (e.g. Rodwell and Folland, 2002), potentially this provides some seasonal predictive skill for regional climate. The NAO determines the intensity and the location of the mid-latitude jet stream, steering the heat and moisture transport from the Atlantic to Europe and forming European climate conditions. Many studies (e.g. Hurrell, 1995; Wibig, 1999; Cassou and Terray, 2001; Gulev et al., 2002) analysed this mechanism for the cold season. Less has been done so far for the analysis of European climate variability during the warm season when zonal heat and moisture transport is diminished and the relative role of local processes in

regional climate variability is increased. As a result, major mechanisms driving European climate variability during the warm season are not well understood. Moreover, these mechanisms might be different for different climatic variables.

Atmospheric water vapour plays a key role both in radiative and dynamic processes of the climate system. It is the most important greenhouse gas, absorbing strongly a portion of the Earth's outgoing thermal energy and radiating a substantial fraction of this energy back to the surface. As water vapour condenses into clouds, cooling effects become important also. The amount of moisture in the atmosphere, is strongly related to air temperature according to the Clausius–Clapeyron equation, and is expected to rise as climate warms thus strengthening the greenhouse effect. Water vapour content is also crucial for precipitation, and through latent heat, is driving dynamical processes in the troposphere. Because of a great number of feedbacks in which water vapour is involved it is a source of strong uncertainty when predicting future climate. That is why during the past two decades, analysis of the spatial-temporal variability of atmospheric moisture has received considerable attention. A number of papers focused on the regional changes in atmospheric water

---

\*Corresponding author.  
e-mail: igorz@sail.msk.ru  
DOI: 10.1111/j.1600-0870.2007.00283.x

vapour (e.g. Flohn and Kapala, 1989; Ross and Elliott, 1996, 2001; Zhai and Eskridge, 1997; Trenberth et al., 2005). Several other studies considered global distribution of the atmospheric moisture and its variability (Oort, 1983; Peixoto and Oort, 1992; Gaffen et al., 1991; Dai, 2006). Although precipitable water (PW) variability is linked to variations of air temperature and precipitation, character and strength of these links vary significantly both in time and space (e.g. Zveryaev and Allan, 2005). Therefore, understanding of mechanisms driving PW variability and its links to other key climatic variables is crucial for correct modelling of the regional hydrological cycle. Thus, along with analysis of major features of PW variability over Europe, examination of the above links for winter and summer seasons is another aim of this study.

In the present study we analyse interannual PW variability over Europe during cold and warm seasons on the basis of relatively continuous-in-time and spatially homogeneous data available from the National Centers for Environmental Prediction/National Center for Atmospheric Research (hereafter NCEP/NCAR) reanalysis (Kalnay et al., 1996). Several studies show that interannual variability of PW is well captured in the NCEP/NCAR reanalysis (Trenberth and Guillemot, 1998; Allan et al., 2002; Sudradjat et al., 2005). Additionally, the NCEP/NCAR reanalysis provides longer records than the ERA40 reanalysis (Uppala et al., 2005), while both produce a similar PW variability over land (Allan, 2007). The data used in the present study and analysis methods are described in Section 2. Characteristics of PW variability during winter and summer seasons for 1979–2004 are described in Section 3. Section 4 examines links between PW variability and regional atmospheric circulation, as well as with some other key climatic variables. Finally, concluding remarks are presented in Section 5.

## 2. Data and methods

The main data source for this study is the NCEP/NCAR reanalysis (Kalnay et al., 1996; Kistler et al., 2001), which uses a frozen assimilation technique to simulate atmospheric conditions at a 6-hourly temporal resolution and 2.5° latitude by 2.5° longitude spatial resolution for a period 1948–present. In our analysis we used monthly PW content (i.e. the total column water vapour; hereafter PW) from NCEP/NCAR reanalysis for 1979–2004. To reveal the dynamical context of the leading PW modes over Europe, we used monthly sea level pressure (hereafter SLP) data and 700 hPa vertical motion fields from the NCEP/NCAR reanalysis (Kalnay et al., 1996) for the period analysed (i.e. 1979–2004).

In the present study we also used indices of the major teleconnection patterns that have been documented and described by Barnston and Livezey (1987). The patterns and indices were obtained by applying rotated principal component analysis to standardized 500 hPa height anomalies over northern hemisphere. These indices are regularly updated and

available from the Climate Prediction Center (CPC) website (<http://www.cpc.ncep.noaa.gov/data/teledoc/telecontents.html>). These data cover the period 1950–present. Details on the teleconnection pattern calculation procedures can be found in Barnston and Livezey (1987) and at the CPC website.

In our study, we consider the climatologies of winter (DJF) and summer (JJA) seasonal mean PW and its standard deviations (STD) as a measure of the total year-to-year variability. To examine spatial-temporal structure of the long-term variations of seasonal mean PW over Europe, we applied empirical orthogonal functions (EOFs) analysis based on the covariance matrix (Wilks, 1995; von Storch and Navarra, 1995). Before the EOF analysis the annual cycle was removed from all grid point time series by subtracting from each seasonal value the respective season's long-term mean. In order to account for the latitudinal distortions, each grid point of the large-scale field anomalies was weighted by the square root of cosine of latitude to ensure that equal areas are afforded equal weight in the analysis (North et al., 1982). The time series has been linearly detrended before the EOF analysis. Spatial patterns and respective principal components (hereafter PCs) of the leading modes of the winter and summer PW are discussed in detail.

We performed singular value decomposition (SVD) of the covariance matrix between seasonal mean PW fields over Europe and the SLP fields in the North Atlantic – European sector. The method of SVD has been developed to extract the dominant covarying modes of variability between two fields (Prohaska, 1976; Bretherton et al., 1992). The SVD technique is a generalization of the EOF analysis (Lorenz, 1956; Davis, 1976). Rather than extracting the modes that explain the greatest variance in a single field, as in EOFs, the SVD techniques finds the covarying modes that explain the greatest covariance between fields. Detailed descriptions of SVD analysis can be found in Bretherton et al. (1992) and von Storch and Navarra (1995). Since SVD analysis has some drawbacks as indicated in Newman and Sardeshmukh (1995) and Cherry (1996), we verified results of the present analysis in two ways. First, we performed SVD analysis on the monthly winter and summer time series (seasonal cycle removed), thus getting essentially longer time series. Results of this additional analysis were very close (both in terms of spatial patterns and squared covariance fractions) to those obtained from analysis of seasonal means. Second, we estimated correlations between principal components of the leading EOFs of PW and SLP fields in the North Atlantic–European sector. Obtained correlation patterns (not shown) appeared very similar to the respective SLP patterns from SVD analysis. Thus, results of our SVD analysis reflect the real relationship between regional PW and SLP fields. To assess links to teleconnection patterns we used conventional correlation analysis. No lead or lag relationships were taken into consideration for this work; our analysis was restricted to simultaneous connections between winter and summer PW fields over Europe and major teleconnection patterns.

### 3. Interannual variability of PW

#### 3.1. Climatologies and standard deviations of the seasonal mean PW

The largest (reaching  $17 \text{ kg m}^{-2}$ ) climatological seasonal mean winter (December–February, hereafter DJF) PW values (Fig. 1a) are observed over the oceanic/marine regions, surrounding Europe (i.e. eastern Atlantic, Bay of Biscay, Mediterranean and Black Seas). These regions are characterized by the large latent heat fluxes during winter. Note PW is significantly lower ( $8\text{--}11 \text{ kg m}^{-2}$ ) over the Baltic and the North Sea. The lowest values of winter PW (less than  $6 \text{ kg m}^{-2}$ ), however, are detected over Scandinavia and northeastern European Russia. The standard deviation (STD) of the time series of the seasonal mean DJF PW is a measure of its total year-to-year variability (Fig. 1a). This variability is the largest (reaching  $1.5 \text{ kg m}^{-2}$ ) over the southern Iberian Peninsula and southwestern Scandinavia, thus, being consistent with the largest variability of the winter precipitation detected in these regions (Zveryaev, 2004) from analysis of the data from the Climate Prediction Center Merged Analysis of Precipitation (hereafter CMAP) data set (Xie and Arkin, 1997).

The smallest magnitudes of the winter PW variability are found over the Alps and the Caucasus in agreement with local minima of climatological PW in these regions. There are two reasons for climatological minima of PW over high mountains. First, the atmospheric layer over mountains is thinner and colder compared to other regions, and therefore can hold less water vapour under the same conditions. Second, much of the water vapour advecting from lower levels is lost via precipitation which is heavy over the orography.

The climatology of the summer (June–August, hereafter JJA) seasonal mean PW and STDs of the corresponding time series over Europe are depicted in Fig. 1b. The largest PW values (reaching  $28 \text{ kg m}^{-2}$ ) are detected over the northwestern Mediterranean, eastern Europe, southern European Russia and the Black Sea regions. Thus, the pattern is essentially different from that for summer precipitation (Zveryaev, 2004) where precipitation maxima were found over the Alps, western Scandinavia and the Caucasus. Spatial structure of year-to-year variability of JJA PW over Europe, presented by its STDs, reveals the largest magnitudes of PW variability over eastern Europe and European Russia (Fig. 1b). Enhanced variability of PW is also detected over the Mediterranean–Black Sea region. Overall

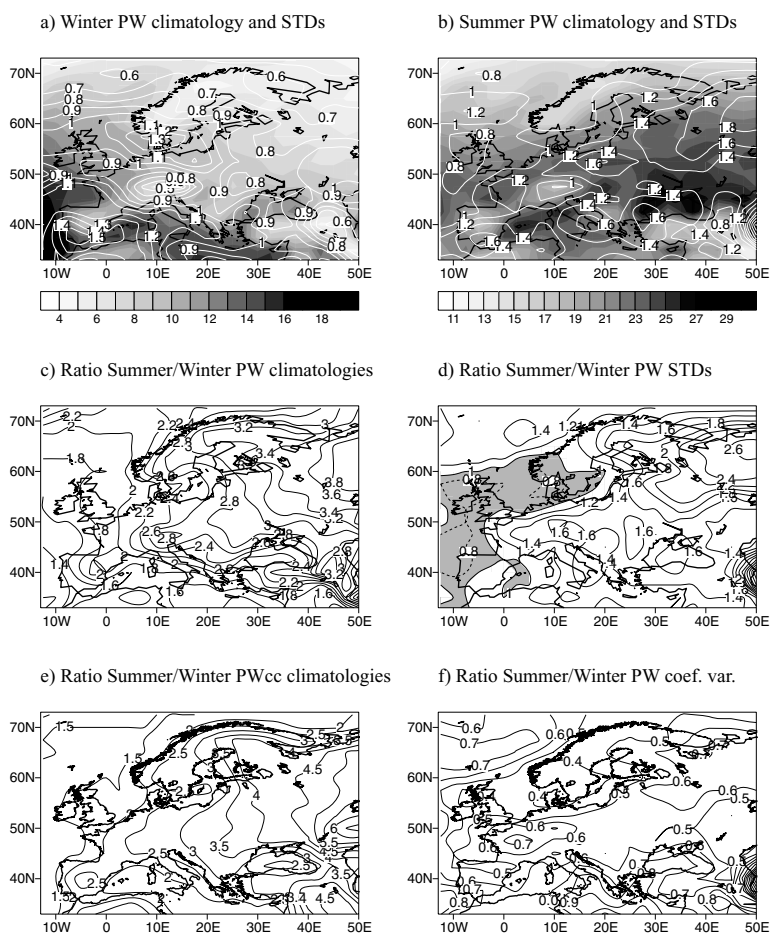


Fig. 1. Climatologies (in shading) and standard deviations (in solid curves) of the winter (a) and summer (b) PW (1979–2004). Ratios between climatologies (c) and standard deviations (d). Ratios between thermodynamic PW components (e) and coefficients of variation (f). Dashed curves and shading in (d) indicate ratio values  $< 1.0$ .

the spatial structure of both climatologies and STDs of summer PW is essentially different from that for the winter season (Fig. 1a).

To emphasize seasonal differences in PW climatologies and STDs we estimated ratios between respective summer and winter characteristics. Figure 1c shows that over the entire domain of analysis, summer PW values are larger than the winter ones. The largest seasonal increase of PW is revealed over European Russia and eastern Scandinavia where the ratio is as high as 3.0–3.8. The increase in ratio from west to east is explained primarily by the thermodynamic relationship between saturated vapour pressure and temperature. To illustrate this point, the PW summer/winter ratio is calculated using a thermodynamic relationship derived over the oceans,  $\ln(\text{PW}) = -14.0 + 0.059T_{1.5}$  (Zveryaev and Allan, 2005), where  $T_{1.5}$  is the NCEP 1.5 m air temperature. Ratios ranging from below 2 over the oceans to above 5 over European Russia (Fig. 1e) are explained by the larger seasonal changes in  $T_{1.5}$  over the continental interior. The expected changes are broadly consistent with the directly calculated values in Fig. 1c, although the theoretical changes are larger to the east, explained by the lack of an open water moisture supply, resulting in reduced summer relative humidity compared to the winter.

Interannual variability of PW over Europe is also intensified significantly during the summer season (Fig. 1d). The largest ratios between summer and winter STDs reach values of 2.0–2.6 over northeastern European Russia and eastern Scandinavia. The smallest seasonal increase of both PW climatologies and STDs is detected over the eastern Atlantic and Mediterranean region. Over some eastern Atlantic regions magnitudes of interannual variability of summer PW are even lower than those of winter PW. We note, however, that revealed seasonal intensification of interannual variability of PW is associated with a seasonal increase of mean PW values. When variability is assessed in terms of coefficients of variation (i.e. standard deviations normalized

by mean values) the ratio between respective summer and winter coefficients shows weaker (compared to the cold season) inter-annual variability of PW during the warm season (Fig. 1f).

### 3.2. Leading modes of PW variability

To reveal the dominant modes of year-to-year variability of PW over Europe and analyse their seasonal differences, we applied EOF analysis to the time series of the seasonal (winter and summer) mean PW. Only the first two EOF modes are separated reasonably well from subsequent modes with respect to sampling errors (North et al., 1982). These two EOFs jointly explain more than 40.0% of the total variance of PW in both seasons. Spatial patterns of the first two EOF modes are presented in Fig. 2. Time series of the respective PCs are depicted in Fig. 3.

The first EOF mode accounts for 34.7% of the total variance of winter mean PW. Its spatial pattern (Fig. 2a) shows two major action centres of opposite polarity with the largest loadings over western Scandinavia and the Iberian peninsula, and reflects opposite DJF PW variations over northern and southern Europe. The pattern is similar to the first EOF mode pattern of the winter precipitation (e.g. Hurrell, 1995; Zveryaev, 2004). The explained variance, however, is lower than that obtained from analysis of CMAP precipitation (42.1%) presented by Zveryaev (2004). The first EOF of winter PW is linked to the major climatic signal in the region—the NAO which drives the wintertime atmospheric moisture transport into European region. The PC-1 (Fig. 3a), displaying temporal behaviour of this mode, demonstrates a close relationship with the winter NAO index ( $R = 0.74$ ).

The second EOF mode explains 17.7% of the total variance of winter PW. The respective spatial pattern (Fig. 2b) depicts coherent PW variations over almost all of Europe, showing the largest loadings over the eastern Europe/western Baltic region. Weak PW variations of opposite sign are detected only over Turkey and

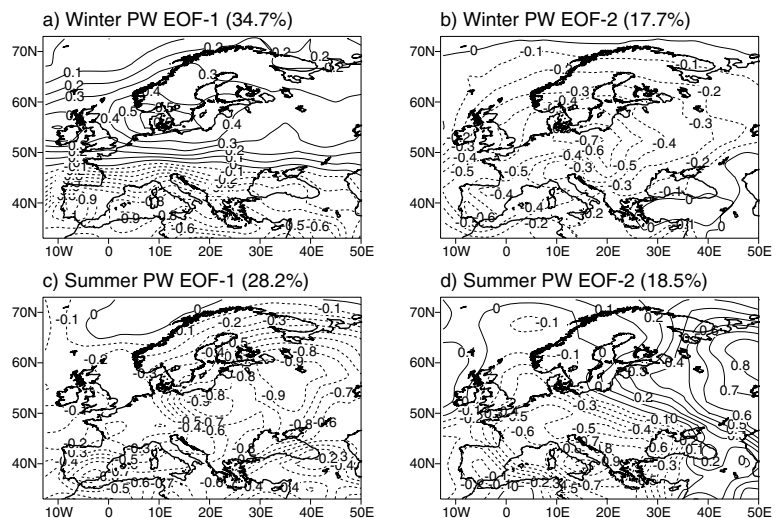


Fig. 2. Spatial patterns of the first (a,c) and second (b,d) EOF modes of winter (a,b) and summer (c,d) PW. Dashed curves indicate negative values. The period of analysis is 1979–2004.

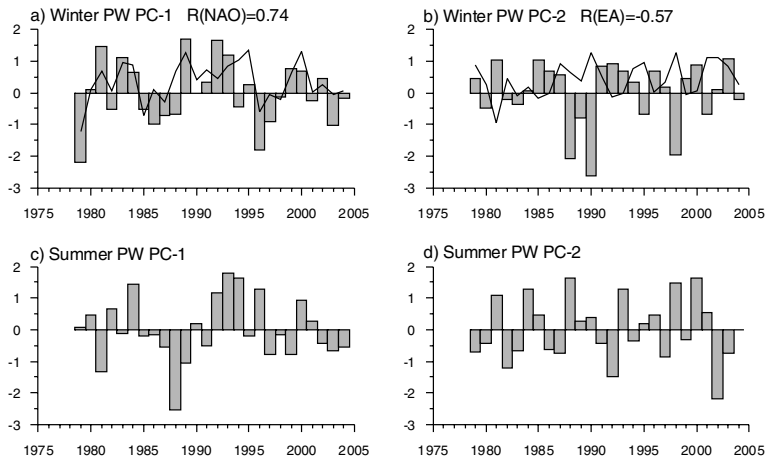


Fig. 3. Principal components of the first (a,c) and second (b,d) EOF modes of winter (a,b) and summer (c,d) PW. Solid curves indicate the NAO (a) and EA (b) indices. The period of analysis is 1979–2004.

the Caucasus region. In contrast to the first EOF mode, this pattern differs significantly from the meridional tripole pattern of the second EOF mode of the winter CMAP precipitation (Zveryaev, 2004). Relatively large ( $R = -0.57$ ) correlation (Fig. 2b) between PC-2 and the index of the East Atlantic (hereafter EA) teleconnection pattern implies association of the second EOF mode of winter PW with this mode of the regional atmospheric circulation. The EA pattern was described (along with other teleconnection patterns) by Barnston and Livezey (1987). Structurally similar to the NAO pattern, the EA pattern is characterized by a meridional dipole with two anomaly centres. However, it is shifted southeastward relative to the NAO dipole. Although the second EOF mode explains a relatively low percentage of winter PW variance, the local effect of this mode might be essential in the regions characterized by the large loadings (e.g. western Baltic region).

During summer the first EOF mode accounts for 28.2% of the total variance of seasonal mean PW. Similar to the second EOF mode of winter PW, the spatial pattern of this mode (Fig. 2c) reflects coherent PW variations over the entire European region. The largest loadings are detected over eastern Europe and European Russia. During recent decades principal components (Fig. 3c) of this mode demonstrate decadal-scale variations with multiyear periods of predominantly positive (1984–1991) and negative (1992–1996) PW anomalies. This feature of decadal scale variability has also been revealed in summer (July–August) time series of sea level pressure over northeast Atlantic presented by Hurrell and Folland (2002) (see their Fig. 1).

The second EOF explains 18.5% of the total variance of summer PW over Europe. Its spatial pattern is characterized by the prominent southwest-northeast oriented dipole (Fig. 2d), with the strongest signal being in the Mediterranean region, and opposite PW variations evident over European Russia and eastern Scandinavia. Principal components of this mode (Fig. 3d) demonstrate interannual variability of summer PW that is not associated with known regional teleconnection patterns. It is worth noting that compared to the principal components of the first

EOF mode (Fig. 3d), PC-2 represents shorter-term interannual variability of summer PW over Europe.

It is interesting to note that the leading EOFs from the present analysis and from analysis of the seasonal mean precipitation (Zveryaev, 2004) are strongly linked during the cold season, and not linked during the warm season. Correlations between respective PCs are 0.91 for winter and 0.16 for summer.

## 4. Links to atmospheric circulation

### 4.1. Leading SVD modes

To explore the links between PW variability over Europe and regional atmospheric circulation, we performed conventional SVD analysis (Bretherton et al., 1992) on the detrended seasonal mean PW and SLP data. Linear coupled dominant modes between fields of PW over Europe and SLP in the North Atlantic—European sector were defined for winter and summer seasons. We limit our analysis to consideration of the first SVD mode only since each of the subsequent modes explains very small fractions of the total covariance of PW and SLP in both seasons. The eigenvalues of the considered SVD modes are well separated from higher-order patterns.

The dominant SVD mode (SVD-1) of covarying winter mean PW and SLP explains 80% of the squared covariance between the fields. The SVD-1 spatial pattern for the winter SLP (Fig. 4a) is characterized by the meridional dipole with the largest loadings over a broad region extending from Greenland to Scandinavia (first action centre), and over the Azores—western Mediterranean region (second action centre with opposite SLP variations). The obtained pattern is typical for the positive phase of NAO that is characterized by below normal SLP in the region around Iceland, and above normal SLP in the extensive region around Azores. This SLP pattern results in anomalous atmospheric moisture advection into the region and excessive (deficient) precipitation over northern (southern) Europe (e.g. Hurrell, 1995; Zveryaev, 2004). The SVD-1 spatial pattern for

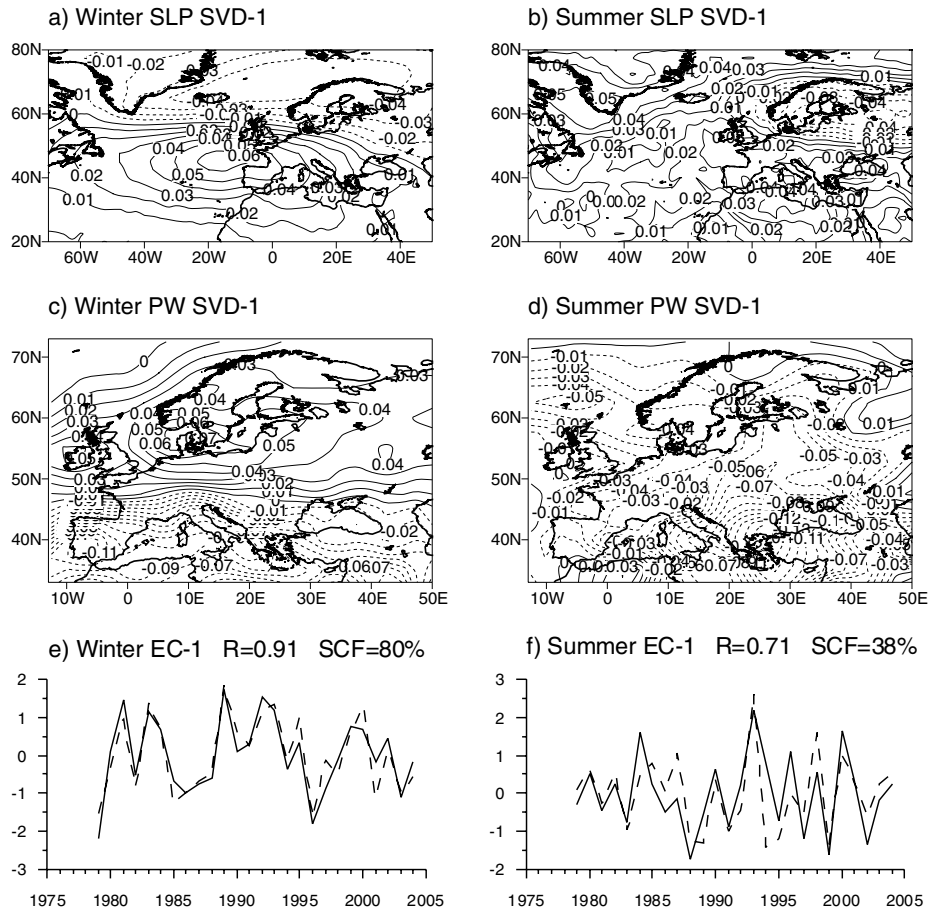


Fig. 4. The SVD-1 mode spatial patterns (a-d) and expansion coefficients (e,f) obtained for pairs of winter (a,c,e) and summer (b,d,f) PW and SLP fields. Expansion coefficients are normalized by their standard deviations. In (a-d) dashed curves indicate negative values. In (e,f) solid (dashed) curve denotes PW (SLP) variations.

winter PW (Fig. 4c) shows opposite PW variations over northern and southern Europe, thus, being consistent with above mentioned NAO-associated winter precipitation pattern over Europe. Time series of expansion coefficients of SLP and PW patterns (Fig. 4a) are strongly linked (correlation is 0.91) to each other and to the winter NAO index (respective correlations are 0.75 and 0.74). Therefore, in accord with earlier studies (e.g. Trigo et al., 2002), our results imply that winter PW variability over Europe is primarily driven by the NAO.

During summer the SVD-1 mode accounts only for 38% of the squared covariance between seasonal mean PW and SLP fields. In general that means relatively weak links between interannual variations of these climatic parameters. The SVD-1 spatial pattern for the summer SLP (Fig. 4b) is characterized by the zonal dipole with the strong PW variations over Scandinavia and northern European Russia (first action centre) and opposite intensive variability of PW over Greenland (second action centre). Thus, this pattern is completely different from the respective winter pattern (Fig. 4a). The associated SVD-1 spatial pattern for summer PW (Fig. 4d) shows coherent PW variations throughout

much of Europe with the largest loadings over southern Europe and Mediterranean region. Note this is somewhat different from the summer EOF-1 pattern of PW (Fig. 2c) where the largest PW variability has been found over European Russia. Also local PW variability of the opposite sign is evident over northeastern European Russia. Correlation (0.71) between time series of expansion coefficients of SLP and PW patterns is essentially lower than that obtained for the winter season (0.91). In general our results suggest a weakening of the role of atmospheric dynamics (moisture advection) in regional PW variability during summer, whereas the role of local processes increases during the warm season. More specifically, convective precipitation comes about through moisture convergence so as PW increases so does the potential moisture supply for convective rain (e.g. Trenberth et al., 2003).

#### 4.2. Summertime links to SLP fields

Since we did not find significant links between leading EOF modes of summer PW over Europe and regional teleconnection

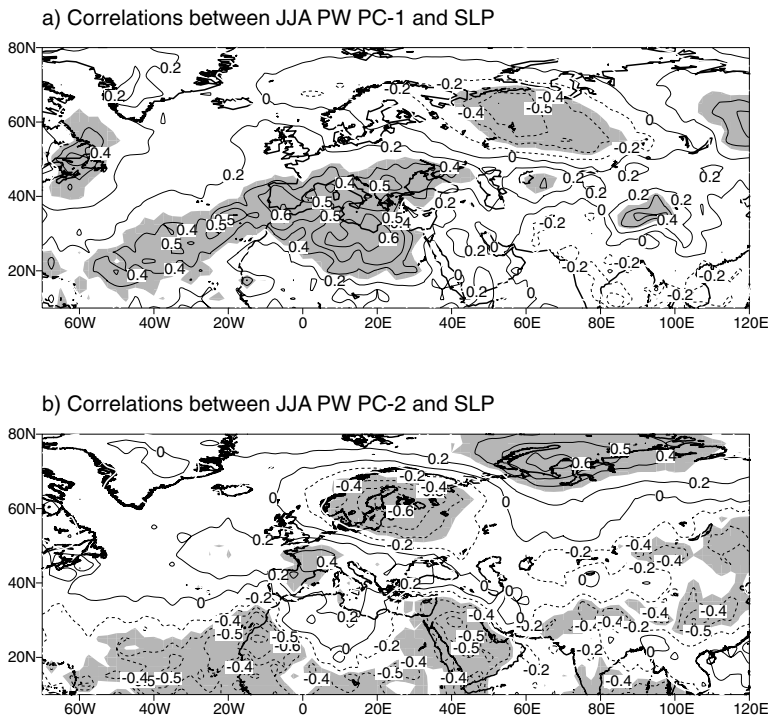


Fig. 5. Correlations between PC-1 (a) and PC-2 (b) of the summer PW and SLP fields. Shaded areas indicate 95% significance level.

patterns and SVD analysis revealed relatively weak association between summertime variability of PW over Europe and SLP in Atlantic-European sector, we extend our analysis to the wider Atlantic-Eurasian region limited to latitudes  $10^{\circ}\text{N}$ – $80^{\circ}\text{N}$  and longitudes  $70^{\circ}\text{W}$ – $120^{\circ}\text{E}$ . Figure 5 depicts correlations between PC-1 and PC-2 of summer PW and SLP fields over this region as well as their local significance at the 95% level according to Student's  $t$ -test (Bendat and Piersol, 1966). It is worth mentioning that the significance level of the correlations might be reduced if the time series are influenced by autocorrelation. Large lag-one autocorrelations reduce significantly effective number of degrees of freedom, whereas influence of small autocorrelations is weak (e.g. Bretherton et al., 1999). In this analysis we have examined the possible impact of autocorrelation on the estimation of significance of correlation coefficients (estimated through the Fisher  $z$ -transform). Neither time series (i.e. PC-1 and PC-2 of summer PW, time series of SLP, air temperature and vertical velocity) considered in the study revealed significant autocorrelations.

Two centres of high and statistically significant correlations between PC-1 of summer PW and SLP are relevant to our analysis (Fig. 5a). The first centre, where correlations reach 0.6, covers an extensive region including southern Europe, the Mediterranean Sea, and a substantial portion of northern Africa. The second centre, showing negative correlation (exceeding  $-0.4$ ) is located over northwestern Siberia. Thus, these two centres form a southwest-northeast oriented dipole, resulting in advection of relatively dry (and cold) air from the northwest into the European region. The above advection of dry air forms negative PW anomalies throughout Europe (Fig. 2c).

Figure 5b shows correlations between PC-2 of summer PW and SLP fields. The largest negative correlations (reaching  $-0.6$ ) are detected over Scandinavia/northeastern European Russia, whereas the largest positive correlations of the same magnitude are found over the northern margin of Siberia and the Kara Sea. Weaker, but statistically significant positive correlations are also found over southwestern Europe. Further southwest the extensive region of significant negative correlations is revealed over the tropical Atlantic. Two of the above correlation centres, namely Scandinavia and southwestern Europe, are responsible for the formation of the EOF-2 dipole pattern of summer PW (Fig. 2d), implying that cyclonic (anticyclonic) circulation anomalies over Scandinavia (southwestern Europe) result in above (below) normal PW in the respective regions. It is worth noting that the entire chain of the above detected centres of high correlations is structurally reminiscent of a Rossby wave pattern emanating from the tropical Atlantic through the European region to the Arctic (Fig. 5b), suggesting possible influence of the tropics on the second EOF mode of summer PW. Note, however, that this mode explains only 18.5% of the summer PW variability in the region.

Because the role of large-scale atmospheric dynamics in regional PW variability diminishes during summer, while the role of local processes increases (e.g. Trenberth, 1999), we examine links to regional air temperature and atmospheric vertical motion. We estimated correlations between PC-1 of summer PW and air temperature from NCEP/NCAR reanalysis. Figure 6a shows large correlations over European Russia and eastern Scandinavia, meaning enhanced (decreased) PW in this region is associated

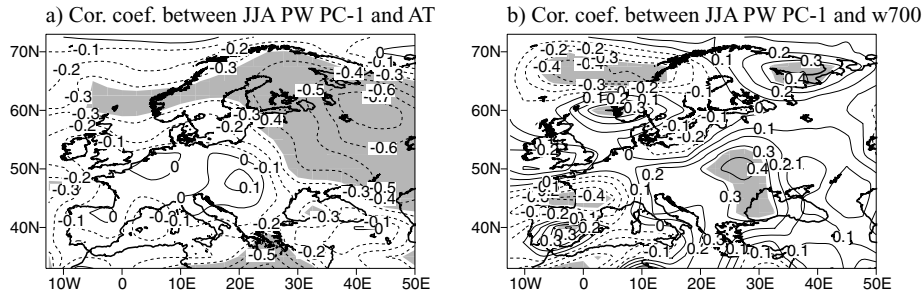


Fig. 6. Correlations between PC-1 of the summer PW and regional surface air temperature (a) and vertical velocity at the 700 hPa level (b). Shaded areas indicate 95% significance level.

with above (below) normal air temperatures. We also examined correlations with vertical velocity at 700 hPa level (Fig. 6b). Although the signal is rather weak, the correlation pattern generally implies that over the region of interest summer PW increase is associated (along with the local heating) with the intensification of upward motion, indicative of low-level moisture convergence. It is worth noting that in the region of our study, convective processes and vertical motion in the atmosphere are not as strong as in the tropical regions (over Maritime continent, for example). Consequently, magnitudes of variability of the respective parameters are not large.

**5. Concluding remarks**

In the present study we analysed climatic variability of the seasonal (winter and summer) mean PW over Europe based on data from the NCEP/NCAR reanalysis (Kalnay et al., 1996). A major seasonal difference in climatologies of PW is that during winter the largest PW values are detected over oceanic/marine regions surrounding Europe, whereas the largest summer PW values are found over land, in particular, over eastern Europe and European Russia. The largest variability (expressed in STDs) of winter PW is attributed to effects of orography (e.g. the Iberian Peninsula, western Scandinavia). The summer PW variability is most intensive over northeastern European Russia. In general, both climatological PW values and STDs over Europe are essentially larger during the boreal summer season. The largest seasonal differences of both characteristics are found over eastern Scandinavia and northeastern European Russia.

Being consistent with results obtained from analysis of regional precipitation variability (Zveryaev, 2004, 2006), the first and second EOFs of winter PW over Europe are associated, respectively, with the NAO and East Atlantic teleconnection patterns. The NAO is the major driver of the winter climate variability over Europe and, therefore, NAO-associated zonal transport of the atmospheric moisture into Europe is crucial in formation of regional anomalies of winter PW.

In contrast to winter, PW variability over Europe during summer is not associated with the NAO (as well as with other regional teleconnection patterns). Moreover, it is not linked with sum-

mer precipitation variability over Europe. Our analysis shows that the first EOF mode of summer PW is associated with SLP pattern characterized by two action centres of opposite polarity. One of them extends over an extensive region from southern Europe to the Mediterranean Sea and northern Africa. Another centre is located over northwestern Siberia. The entire pattern implies advection of relatively dry and cold oceanic/marine air from the northwest into Europe. Note, the principal difference from the winter season is that the enhanced transport of the oceanic/marine air during summer results in negative PW anomalies over Europe, suggesting, along with the strong links to regional air temperature variations, the important role of intense summer heating and associated local convective processes in formation of positive PW anomalies when horizontal moisture transport is diminished. In general, our results are in line with the findings of Trenberth (1999), showing significant seasonal (from cold to warm season) increase of the ‘moistening efficiency’ (i.e. the fraction of moisture evaporated from a region to that flowing through) in the northern hemisphere extra-tropics.

Our analysis did not reveal significant links between the second EOF mode of summer PW over Europe and known regional teleconnection patterns. However, we found that this mode is associated with cyclonic/anticyclonic SLP anomalies over Scandinavia and southwestern Europe. From wider perspective it is worth mentioning that the second EOF mode of summer PW can be influenced by the processes in the tropical Atlantic through Rossby waves emanating from this region. This possible link, however, needs further investigation.

An important feature of seasonality in regional PW variability, revealed in the study, is that during the cold season PW variability is strongly coupled with the variability of precipitation, which is not the case for the warm season. Instead, during the warm season we found rather strong link between regional PW and air temperature.

Summarizing results of the present study we note that this is the first time the seasonal PW variability over Europe has been studied in reanalyses, focusing on the contrasts in regional PW variability between cold and warm seasons. Our results highlight essential seasonality in characteristics of PW variability over Europe. Moreover, the present study reveals differing physical

mechanisms that drive regional PW variability during cold and warm seasons. While wintertime PW variability is well studied and generally well understood, analysis of the more complicated variability of summer PW deserves further investigation. In particular, analysis (based on observations and model simulations) of the relative role of local convective processes in summer PW variability over Europe looks very promising.

## 6. Acknowledgments

This research was supported by a Marie Curie International Fellowship within the 6th European Community Framework Programme through the contract MTKD-CT-2004-014222. Major part of the present study has been performed during IIZ work at the Department of Meteorology and Climatology of the University of Łódź under the fellowship. IIZ was also supported by the Russian Foundation for Basic Research Grant 05-05-64908 and the NATO SfP project 981044. RPA was supported by a United Kingdom NERC grant NE/C51785X/1. The NCEP data was extracted from NOAA-CIRES Climate Diagnostics Center. The manuscript was improved by the constructive comments of the two anonymous reviewers.

## References

- Allan, R. P. 2007. Improved simulation of water vapour and clear-sky radiation using 24 hour forecasts from ERA40. *Tellus* **59A**, 336–343.
- Allan, R. P., Slingo, A. and Ramaswamy, V. 2002. Analysis of moisture variability in the European Centre for Medium-Range Weather Forecasts 15-year reanalysis over tropical oceans. *J. Geophys. Res.* **107**, 4230, doi: 10.1029/2001JD001132.
- Barnston, A. G. and Livezey, R. E. 1987. Classification, seasonality and persistence of low-frequency atmospheric circulation patterns. *Mon. Wea. Rev.* **115**, 1083–1126.
- Bendat, J. S. and Piersol, A. G. 1966. *Measurement and Analysis of Random Data*. J. Wiley & Sons, New York, 390 pp.
- Bretherton, C. S., Smith, C. and Wallace, J. M. 1992. An intercomparison of methods for finding coupled patterns in climate data. *J. Climate* **5**, 541–560.
- Bretherton, C. S., Widmann, M., Dymnikov, V. P., Wallace, J. M. and Blade, I. 1999. The effective number of spatial degrees of freedom of a time-varying field. *J. Climate*. **12**, 1990–2009.
- Cassou, C. and Terray, L. 2001. Oceanic forcing of the wintertime low-frequency atmospheric variability in the North Atlantic European sector: a study with the APREGÉ model. *J. Climate*. **14**, 4266–4291.
- Cherry, S. 1996. Singular value decomposition analysis and canonical correlation analysis. *J. Climate*. **9**, 2003–2009.
- Dai, A. 2006. Recent climatology, variability and trends in global surface humidity. *J. Climate* **19**, 3589–3606.
- Davis, R. 1976. Predictability of sea surface temperature and sea level pressure anomalies over the North Pacific Ocean. *J. Phys. Oceanogr.* **6**, 246–266.
- Flohn, H. and Kapala, A. 1989. Changes of tropical sea-air interaction processes over a 30-year period. *Nature* **338**, 244–246.
- Gaffen, D. J., Barnett, T. P. and Elliott, W. P. 1991. Space and time scales of global tropospheric moisture. *J. Climate* **4**, 989–1008.
- Gulev, S. K., Jung, T. and Ruprecht, E. 2002. Interannual and seasonal variability in the intensities of synoptic scale processes in the North Atlantic mid latitudes from the NCEP/NCAR Reanalysis data. *J. Climate* **15**, 809–828.
- Hurrell, J. W. 1995. Decadal trends in the North Atlantic oscillation: regional temperature and precipitation. *Science* **269**, 676–679.
- Hurrell, J. W. and Folland, C. K. 2002. A change in the summer atmospheric circulation over the North Atlantic. *CLIVAR Exch.* **7**(3–4), 52–54.
- Kalnay, E., Kanamitsu, M., Kistler, R., Collins, W., Deaven, D. and co-authors. 1996. The NCEP/NCAR 40-year reanalysis Project. *Bull. Amer. Met. Soc.* **77**(3), 437–471.
- Kistler, R., Collins, W., Saha, S., White, G., Wollen, and co-authors. 2001. The NCEP/NCAR 50-year reanalysis: monthly means CD-ROM and documentation. *Bull. Amer. Met. Soc.* **82**(2), 247–268.
- Lorenz, E. 1956. Empirical orthogonal functions and statistical weather prediction. Statistical Forecasting Project Rep. 1, Dept. of Meteorology, Massachusetts Institute of Technology, 49 pp. [NTIS AD-110-268.
- Newman, M. and Sardeshmukh, P. D. 1995. A caveat concerning singular value decomposition. *J. Climate* **8**, 352–360.
- North, G. R., Bell, T. L. and Calahan, R. F. 1982. Sampling errors in the estimation of empirical orthogonal functions. *Mon. Wea. Rev.* **110**, 699–706.
- Oort, A. H. 1983. Global atmospheric circulation statistics, 1958–1973. NOAA Prof. Pap. 14, 180 pp. [Available from U.S. Govt. Printing Office, Washington, DC 20402.
- Peixoto, J. P. and Oort, A. H. 1992. *Physics of Climate*. American Institute of Physics, 520 pp.
- Prohaska, J. 1976. A technique for analyzing the linear relationships between two meteorological fields. *Mon. Wea. Rev.* **104**, 1345–1353.
- Rodwell, M. J. and Folland, C. K. 2002. Atlantic air-sea interaction and seasonal predictability. *Q. J. R. Meteorol. Soc.* **128**, 1413–1443.
- Rogers, J. C. 1984. The association between the North Atlantic Oscillation and the Southern Oscillation in the northern hemisphere. *Mon. Wea. Rev.* **112**, 1999–2015.
- Ross, R. J. and Elliott, W. P. 2001. Radiosonde-based Northern Hemisphere tropospheric water vapor trend. *J. Climate* **14**, 1602–1612.
- Ross, R. J. and Elliott, W. P. 1996. Tropospheric Water Vapor Climatology and Trends over North America: 1973–93. *J. Climate* **9**, 3561–3574.
- Seager, R., Kushnir, Y., Visbek, M., Naik, N., Miller, J., Krahnmann, G. and Cullen, H. 2000. Causes of Atlantic Ocean climate variability between 1958 and 1998. *J. Climate*. **13**, 2845–2862.
- Sudradjat, A., Ferraro, R. R. and Fiorino, M. 2005. A comparison of total precipitable water between reanalyses and NVAP. *J. Climate* **18**, 1790–1807.
- Trenberth, K. E. 1999. Atmospheric moisture recycling: role of advection and local evaporation. *J. Climate* **12**, 1368–1381.
- Trenberth, K. E., Dai, A., Rasmussen, R. M. and Parsons, D. B. 2003. The changing character of precipitation. *Bull. Am. Meteorol. Soc.* **84**, 1205–1217.
- Trenberth, K. E., Fasullo, J. and Smith, L. 2005. Trends and variability in column-integrated atmospheric water vapor. *Clim. Dyn.* **24**, 741–758.

- Trenberth, K. E. and Guillemot, C. J. 1998. Evaluation of the atmospheric moisture and hydrological cycle in the NCEP/NCAR reanalyses. *Clim. Dyn.* **14**, 213–231.
- Trigo, R. M., Osborn, T. J. and Corte-Real, J. M. 2002. The North Atlantic Oscillation influence on Europe: climate impacts and associated physical mechanisms. *Clim. Res.* **20**, 9–17.
- Uppala, S. M., Kållberg, P. W., Simmons, A. J., Andrae, U., Da Costa Bechtold, V. and co-authors. 2005. The ERA-40 Re-analysis. *Q. J. Roy. Meteorol. Soc.* **131**, 2961–3012.
- van Loon, H. and Rogers, J. C. 1978. Seesaw in winter temperatures between Greenland and Northern Europe, I, General description. *Mon. Wea. Rev.* **106**, 296–310.
- von Storch, H. and Navarra, A. 1995. *Analysis of Climate Variability*. Springer-Verlag, New-York, 334 pp.
- Wibig, J. 1999. Precipitation in Europe in relation to circulation patterns at the 500 hPa level. *Int. J. Climatol.* **19**, 253–269.
- Wilks, D. S. 1995. *Statistical Methods in the Atmospheric Sciences*. Academic Press, New York, 467 pp.
- Xie, P. and Arkin, P. 1997. Global precipitation: a 17-year monthly analysis based on gauge observations, satellite estimates, and numerical model outputs. *Bull. Amer. Meteorol. Soc.* **78**, 2539–2558.
- Zhai, P. and Eskridge, R. E. 1997. Atmospheric water vapour over China. *J. Climate* **10**, 2643–2652.
- Zveryaev, I. I. 2004. Seasonality in precipitation variability over Europe. *J. Geophys. Res.* **109**, D051103, doi:10.1029/2003JD003668.
- Zveryaev, I. I. 2006. Seasonally varying modes in long-term variability of European precipitation during the 20th century. *J. Geophys. Res.* **111**, D21116, doi:10.1029/2005JD006821.
- Zveryaev, I. I. and Allan, R. P. 2005. Water vapor variability in the tropics and its links to dynamics and precipitation. *J. Geophys. Res.* **110**, D21112, doi:10.1029/2005JD006033.